Applied Physics Letters

Controlling the surface photovoltage on WSe_2 by surface chemical modification

Cite as: Appl. Phys. Lett. **112**, 211603 (2018); https://doi.org/10.1063/1.5026351
Submitted: 19 February 2018 . Accepted: 13 May 2018 . Published Online: 24 May 2018

Ro-Ya Liu, Kenichi Ozawa, Naoya Terashima, Yuto Natsui, Baojie Feng, Suguru Ito, Wei-Chuan Chen, Cheng-Maw Cheng, Susumu Yamamoto, Hiroo Kato, Tai-Chang Chiang, and Iwao Matsuda

Controlling the surface photovoltage on WSe_2 by surface chemical modification

Ro-Ya Liu,[1,2,3] Kenichi Ozawa,[4] Naoya Terashima,[5] Yuto Natsui,[5] Baojie Feng,[6] Suguru Ito,[1] Wei-Chuan Chen,[7] Cheng-Maw Cheng,[7] Susumu Yamamoto,[1] Hiroo Kato,[5] Tai-Chang Chiang,[3] and Iwao Matsuda[1,a)]

[1]*Institute for Solid State Physics, The University of Tokyo, Chiba 277-8581, Japan*
[2]*Institute of Physics, Academia Sinica, Taipei 11529, Taiwan*
[3]*Department of Physics, University of Illinois at Urbana-Champaign, Urbana, Illinois 61801-3080, USA*
[4]*Department of Chemistry, Tokyo Institute of Technology, Tokyo 152-8551, Japan*
[5]*Department of Advanced Physics, Hirosaki University, Aomori 036-8561, Japan*
[6]*Hiroshima Synchrotron Radiation Center, Hiroshima University, 2-313 Kagamiyama, Higashi-Hiroshima 739-0046, Japan*
[7]*National Synchrotron Radiation Research Center, Hsinchu 30076, Taiwan*

(Received 19 February 2018; accepted 13 May 2018; published online 24 May 2018)

The surface photovoltage (SPV) effect is key to the development of opto-electronic devices such as solar-cells and photo-detectors. For the prototypical transition metal dichalcogenide WSe_2, core level and valence band photoemission measurements show that the surface band bending of pristine cleaved surfaces can be readily modified by adsorption with K (an electron donor) or C_{60} (an electron acceptor). Time-resolved pump-probe photoemission measurements reveal that the SPV for pristine cleaved surfaces is enhanced by K adsorption, but suppressed by C_{60} adsorption, and yet the SPV relaxation time is substantially shortened in both cases. Evidently, adsorbate-induced electronic states act as electron-hole recombination centers that shorten the carrier lifetime. *Published by AIP Publishing.* https://doi.org/10.1063/1.5026351

Crystals of transition metal dichalcogenides (TMDCs) are composed of two-dimensional (2D) layers that are bonded with neighbors by the weak van der Waals (vdW) interaction. Such 2D layered materials have been identified as promising components for vdW heterostructure devices.[1] The concept of the vdW heterostructure has been further extended from TMDC layers to metal/TMDC or organic molecules/TMDC layers.[2] WSe_2, one of the TMDC semiconductors, is known to exhibit a large surface photovoltage (SPV) effect,[3] and it has been reported that an even higher SPV is induced by deposition of metals (Rb and In).[4,5] On the other hand, an organic/TMDC heterojunction (C_{60}/MoS_2) has been predicted to show a high quantum yield and a high photovoltaic efficiency for solar cell applications.[2] Concerning opto-electronic devices, the most fundamental optical response is the generation of photovoltage by the spatial separation of the photo-excited electrons and holes that are created at the surface or the interface region. To make further progress, it is important to perform a detailed study of the surface/interface electronic states and its carrier dynamics.

In this study, time-resolved x-ray photoemission spectroscopy (TRXPS) experiments were performed on WSe_2 to investigate carrier dynamics in relation to the SPV effect. The same measurements were carried out for the surfaces after depositions of potassium (K) atoms or fullerene (C_{60}) molecules. The resulting photoemission band diagrams allow us to draw conclusions about the electronic states and the carrier dynamics at the pristine and modified surfaces, and the derived basic knowledge will be useful for developing TMDC heterojunctions. Figures 1(a) and 1(b) show schematic drawings of the atomic structure. The clean surface of WSe_2 was obtained by cleavage in an ultrahigh vacuum chamber. A metal/WSe_2 surface was prepared by depositing ~1 ML potassium on the clean surface with a SAES Getters dispenser at room temperature (RT) while an organic molecule/WSe_2 surface was assembled by depositing ~0.8 ML fullerene on it with a K-cell evaporator at RT. The coverage calibration is explained in the supplementary material.

Photoemission band mapping was performed by angle-resolved photoemission spectroscopy (ARPES) using synchrotron radiation (SR) at beamline 21B of Taiwan Light Source, National Synchrotron Radiation Research Center. The spectra were recorded using a hemispherical analyzer with an energy resolution of 50 meV at photon energies $h\nu = 28$ and 42 eV. TRXPS measurements were carried out at BL07LSU at SPring-8 by the pump-probe method.[6,7] The pump light was a laser pulse of $h\nu = 1.55$ eV with a pulse duration of 60 fs and a pulse interval of 4.79 μs. The probe light was provided by SR pulses of $h\nu = 253$ eV that were generated by F-mode operation of the storage ring with a pulse duration of 50 ps. TRXPS data were obtained using a time-of-flight analyzer. All the photoemission measurements were performed at RT.

Figures 1(d)–1(i) show the changes of core level spectra after surface modifications. After K deposition, both W 4*f* and Se 3*d* spectra indicate an energy shift of 0.18 eV toward higher binding energies as shown in Figs. 1(d) and 1(e), respectively. As shown in Fig. 1(f), the appearance of the K 3*p* peak confirms the presence of the K overlayer. Figures 1(g)–1(i) show the results for C_{60} deposition. The W 4*f* and Se 3*d* core levels show an energy shift of 0.08 eV to the

a)Electronic mail: imatsuda@issp.u-tokyo.ac.jp

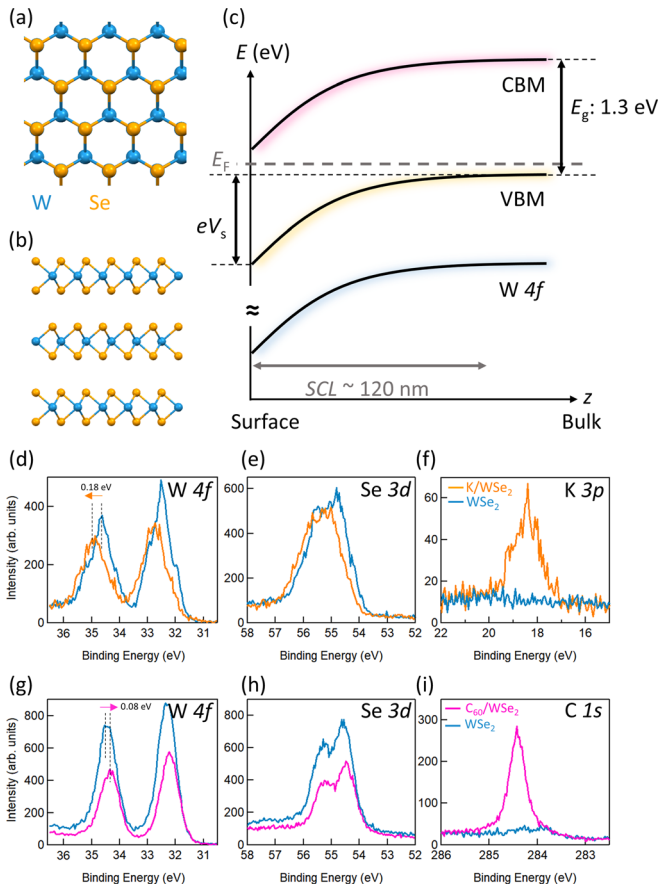

FIG. 1. (a) Top and (b) side views of the WSe_2 atomic structure. (c) Schematic diagram of the surface band bending. (d) and (g) W 4*f*, (e) and (h) Se 3*d*, (f) K 3*p*, and (i) C 1*s* core-level spectra of the pristine WSe_2 surface (blue) and the surfaces covered with K (orange) or C_{60} (pink). The spectra were taken at room temperature at the photon energy of $h\nu = 253$ eV.

lower binding energies, while the C 1*s* core-level confirms the presence of C_{60} adsorbates. Since photoemission spectroscopy probes the near-surface region ($h\nu = 253$ eV), the energy shifts of the core levels correspond to variations of the band-bending effect by adsorbates[2,10,11] and indicate the opposite roles of the two overlayers in modifying bulk states near the surface region or the space-charge layer (SCL).

Figures 2(a)–2(f) show ARPES maps of the valence bands of (a) the pristine WSe_2 surface, (b) the K-covered WSe_2 surface (K/WSe_2), and (c) the C_{60}-covered WSe_2 surface (C_{60}/WSe_2). In Fig. 2(a), dispersion curves of the two bulk valence bands, labeled as VB1 and VB2, reach $\overline{K}$ at $E - E_F$ of -1.26 eV and -1.75 eV, respectively. The valence band maximum (VBM) of the clean WSe_2 surface is thus located at $E - E_F = -1.26$ eV. Since the bulk bandgap of WSe_2 is 1.3 eV,[15] the Fermi level is located very close to the conduction band minimum (CBM), and the surface has an *n*-type band structure. On the other hand, the VBM within the interior of the sample, VBM_{bulk}, is evaluated to be $E - E_F = -0.22$ eV (*p*-type, see supplementary material for further details) for the current sample; thus, there is a built-in surface band bending of $V_s = 1.04$ eV in the sample that gives rise to a space-charge layer or a natural p-n junction [see Fig. 1(c)]. With K deposition, VB1 and VB2 shift to higher binding energies by 0.18 eV, as evaluated from the results in Figs. 2(a) and 2(b). This change is consistent with the shift seen in Figs. 1(d) and 1(e). On the other hand, deposition of C_{60} causes the VBM to move toward a lower binding energy, as seen in Figs. 1(g) and 1(h). The spectral features of VB1 and VB2 appeared faint in Fig. 2(c) due to the C_{60} overlayer, which strongly attenuates the photoemission signal from the substrate at the photon energy of 28 eV used for the measurement.

The observed *p*-type band bending of the pristine WSe_2 surface counters our expectation that a pure crystal of WSe_2 should exhibit flat bands due to the absence of intrinsic surface states on the prefect vdW crystal surface.[11,12] However, previous ARPES studies have also revealed similar surface band bending effects. It has been argued that the actual surfaces might have various types of defects, such as atomic steps or dislocations.[3] Buck *et al.*[4] reported that these factors induce the large band-bending effect and the SCL width of

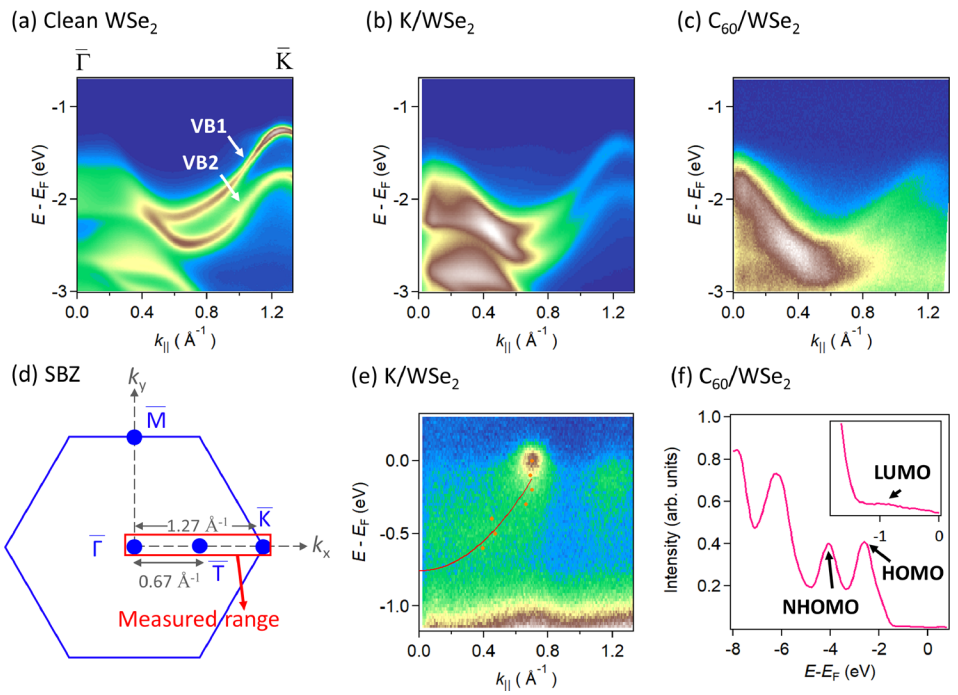

FIG. 2. Photoemission band diagrams of surfaces of (a) WSe_2 (b) K/WSe_2, and (c) C_{60}/WSe_2 taken along the $\overline{\Gamma} - \overline{K}$ axis at (a) $h\nu = 42$ eV, (b) $h\nu = 42$ eV, and (c) $h\nu = 28$ eV. (d) Measured $k_{||}$ range in SBZ. (e) Selected region for K/WSe_2. (f) Angle-integrated spectra of C_{60}/WSe_2 taken at $h\nu = 28$ eV. In the figure, peaks assigned to the molecular orbitals are labeled.

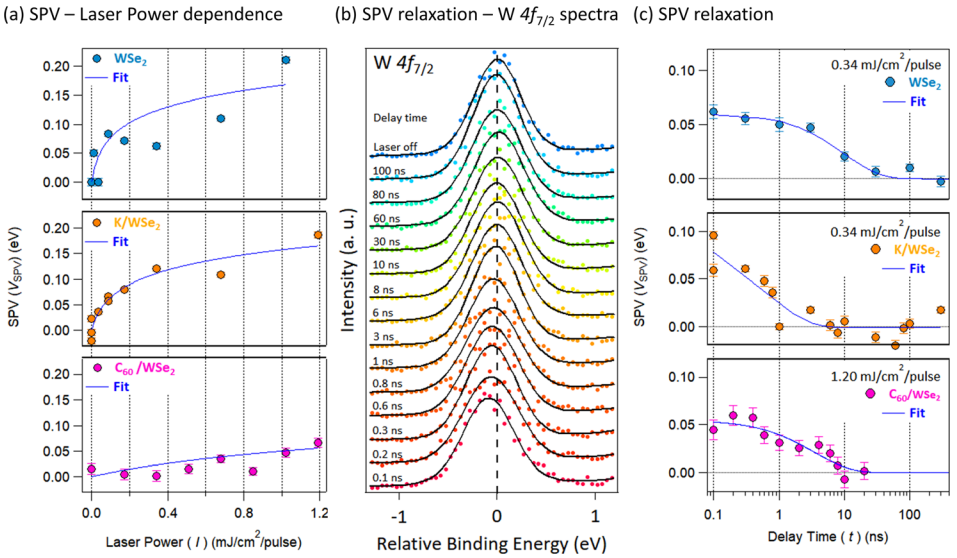

FIG. 3. (a) Energy shifts in the W 4*f* core-level in spectra of WSe_2 (blue), K/WSe_2 (orange), and C_{60}/WSe_2 (pink), as functions of the pumping laser power. The data were recorded at the delay time of 0.1 ns. The power-dependence of the individual surfaces is curve-fitted as blue curves by Eq. (1). (b) A collection of time-resolved W $4f_{7/2}$ core-level spectra of the K/WSe_2 surface taken by the pump ($h\nu = 1.55$ eV) and probe ($h\nu = 253$ eV) method. The pulse energy of the pump was 0.34 mJ/cm^2 per pulse. The spectra (circles) are fitted by Voigt functions (solid lines). (c) Temporal variations of the surface photovoltage (SPV) for WSe_2 (blue), K/WSe_2 (orange), and C_{60}/WSe_2 (pink). Blue curves are the fitting results of Eq. (2).

WSe_2 extends to ~120 nm. The WSe_2 SCL has now attracted much interest as a carrier reservoir for photovoltaics.

Focusing on the photoemission map of K/WSe_2 near the Fermi level [Fig. 2(e)], an apparent spot at $k_{||} = 0.65$ Å^{-1} and a broad dispersive feature are observed in the spectra. The former can be assigned to the CBM located at $\overline{\Gamma}$ [Fig. 2(d)] of WSe_2, while the latter likely arises from a K-derived metallic band. The K-derived electronic state can be regarded as a quantum-well state (QWS)[13] in the overlayer and gives rise to a parabolic dispersion near the Brillouin zone center [Fig. 2(e)]. This assignment is consistent with previous studies[13] and the fact that no K intercalation appeared between the WSe_2 layers[8] [see Fig. 1(f)]. The K overlayer behaves as an electron donor to the WSe_2 layer.

For C_{60}/WSe_2, the highest occupied molecular orbital (HOMO) and the next highest occupied molecular orbital (NHOMO) of the fullerene are observed at $E - E_F = -2.62$ and -4.06 eV, respectively, in the ARPES spectrum [Fig. 2(f)]. The LUMO position of the C_{60} molecule is estimated to be around -1.02 eV.[14] The spectral feature of LUMO can be specified from the gentle slope, as shown in the inset of Fig. 2(f). Comparing the clean surface data shown in Fig. 2(a) with the C_{60} deposited surface data shown in Fig. 2(c), the LUMO level is located within the bandgap of WSe_2 and the energy position of HOMO is lower than the VBM of WSe_2. It is likely that the LUMO orbital is responsible for the acceptor-type[9] character of the C_{60} overlayer on WSe_2. The LUMO position is above the VBM but below E_F, and this is supported by a previous model suggested by a photoluminescence study.[9]

To probe the dynamical behavior of the WSe_2, K/WSe_2, and C_{60}/WSe_2 surfaces, we carried out TRXPS measurements of the W 4*f* core level by the pump-probe method. In the experiment, electron carriers are photo-excited by the ultrafast laser pulses of $h\nu = 1.55$ eV that is larger than the indirect bandgap (1.3 eV).[10,15] Figure 3(a) shows the energy shifts of the core-level peaks by the SPV effect with respect to the power density of the pump pulses. At a pump power density of 1 mJ/cm^2/pulse, the measured photovoltage is about 0.15 V for both K/WSe_2 and WSe_2 and about 0.05 V for C_{60}/WSe_2. Figure 3(b) shows the W$4f_{7/2}$ XPS spectra of K/WSe_2 at different delay times. The time evolution of the SPV is obtained from the energy difference between the peak position as a function of the delay time and the peak position measured at equilibrium (without pump laser). Figure 3(c) displays SPV as a function of delay times for WSe_2, K/WSe_2, and C_{60}/WSe_2. Evidently, the relaxation time for the SPV is different for the three cases, suggesting differences in the dynamical behavior.[16,17]

Conventionally, SPV relaxation can be described by the thermionic emission model[18–20] if thermionic emission dominates the carrier recombination process. The illumination power dependence and the temporal relaxation derived from the rate equation of hole (electron) charge density and the relation between SPV and hole (electron) density are as follows:

$$\begin{cases} V_{SPV}(I) = \eta k_B T \ln(1+\gamma I), & (1) \\ V_{SPV}(t) = -\eta k_B T \ln\left\{1 - \left[1 - \exp\left(-\dfrac{|V_0|}{\eta k_B T}\right)\right] e^{-\frac{t}{\tau_\infty}}\right\}, & (2) \end{cases}$$

where k_B, T, and V_0 are the Boltzmann constant, the sample temperature, and the SPV shift at $t = 0$. I and t are the fluence of the pump laser and the delay time between pump and probe pulses. Parameters η, γ, and τ_∞, are the ideality factor, the efficiency of the optical excitation, and the relaxation time of SPV. The data points in Figs. 3(a) and 3(c) are well fitted by Eqs. (1) and (2). Table I shows a summary of the fitting parameters for WSe_2, K/WSe_2, and C_{60}/WSe_2. The prefactor of η was around 2 for the three surfaces. The quantity η is related to a ratio of thermal cross-section for electrons and holes, and it typically ranges between 0.5 and 2, indicating appropriateness of the model.[19] The relaxation time, τ_∞, of WSe_2 was longer than those of K/WSe_2 and C_{60}/WSe_2, suggesting a faster electron-hole pair recombination rate caused by the overlayers.

Electronic states at surfaces play various roles in controlling the performance of photovoltaic materials. One is to change the degree of band bending that is directly linked to the spatial separation of the photo-excited carriers or generation of photovoltage. The other is to regulate the recombination process of the

TABLE I. SPV shift at t_0 (V_0), ideality factor (η), efficiency of the optical excitation (γ), SPV relaxation times (τ_∞), surface potential barrier heights (V_s), widths of the space charge layer (W), and surface recombination velocity (S).

	V_0 (meV)	η	γ (cm^2/mJ)	τ_∞ (ns)	V_s (eV)	W (nm)	S (m/s)
WSe_2	60 ± 5	1.7 ± 0.9	53 ± 22	16 ± 6	1.04	120	7.5
1 ML K/WSe_2	147 ± 57	1.81 ± 0.43	31.0 ± 20.5	1.2 ± 0.3	1.22	128	107
0.8 ML C_{60}/WSe_2	55 ± 6	1.9 ± 2.2	3.1 ± 6.2	5.5 ± 1.0	0.96	114	21

photo-excited electron-hole pairs. A heterojunction of WSe_2 with the donor-type (K) overlayer enhances the surface potential such that SPV also increases relative to that of the pristine WSe_2 surface at lower pumping laser power density. This may be attributed to the fact that the space charge layer near the surface now includes a region with electron occupation in the conduction band. The electrostatic potential becomes constant within this region, and there is no drift force within to drive the photo-exited carriers. Concerning the relaxation time, τ_∞ was suppressed after K deposition. When the WSe_2 surface makes contact with the acceptor-type (C_{60}) overlayer, the surface potential and the SPV are both reduced, as shown in Figs. 1(g), 1(h), and 3. Furthermore, the relaxation time becomes short, compared to the pristine WSe_2 surface.

In order to describe the different relaxation times by the surface modification, we recall the surface recombination model that approximates the SPV relaxation time as[19,20] $\tau_\infty = \tau_s \sim \frac{W}{S}$, where τ_s, W, and S are the surface recombination time, width, and surface recombination velocity, respectively. The SCL widths for our WSe_2, K/WSe_2, and C_{60}/WSe_2 are evaluated to be about 120 nm from the value of the band bending. Thus, variations in W are not the key factor of the significant changes in relaxation time. On the other hand, the surface recombination velocity can vary with the trapped states at a surface having the 2D density. The surface recombination velocity can be written as[21,22] $S = N_t v_{th} \sigma_p e^{-eV_s/\eta k_B T}$, where N_t, v_{th}, σ_p, and V_s are the trapped carrier density near surfaces, the thermal carrier velocity, the hole carrier capture cross-section, and the surface potential, respectively. The parameters N_t, σ_p, and V_s can vary with surface modifications, but v_{th} should remain as a constant. In this study, V_s changes within ±20% in three of the surfaces (see Table I); thus, the key factors are the density of trapped states and the hole carrier capture cross-section. It is inferred that the QWS and the occupied bulk state near CBM at the K/WSe_2 surface, as observed in Fig. 2(e), may become recombination centers, leading to an increase in N_t or σ_p. In the K/WSe_2 case, one may conclude that the increase in charges (states) at a surface enhances the band-bending effect but it may also enhance the electron-hole pair recombination rate. Concerning the case of C_{60}/WSe_2, the system also has shorter relaxation time than that of the pristine WSe_2 surface. It can be explained by the decrease in V_s [Fig. 1(g)] and the increase in N_t or σ_p [Fig. 2(f)]. The LUMO states located within the bulk bandgap of WSe_2 likely dominate the recombination of the photo-excited electron-hole pairs.

Photoemission band mapping and time-resolved photoelectron spectroscopy were systematically performed on surfaces of a p-type WSe_2 crystal and the modified surfaces with two types of adsorbates, K and C_{60}. For the K/WSe_2 surface, the potassium layer acts as a donor and it enhances the band-bending effect, while the fullerene layer at C_{60}/WSe_2 behaves as an acceptor and it reduces the effect. Transient surface photovoltage effects were observed for the three surfaces. The larger SPV is observed on K/WSe_2 due to the larger initial band bending. The shorter SPV relaxation time after the formation of the overlayers indicates that adsorbate-induced electronic states likely become recombination centers of photo-excited carriers. This system offers a good model to illustrate a trade-off between the magnitude of the SPV and the SPV relaxation rate and the multi-parameter dependencies of SPV generation and relaxation. These observations should provide critical insights into designing TMDC-based optoelectronic devices in the future.

See supplementary material for the coverage estimation of C_{60} and K at the WSe_2 surface and the band bending profile and the space charge layer of p-type WSe_2.

This work was supported by the Grant-in-Aid for Scientific Research (KAKENHI) (Grant Nos. 16H03867 and 16H06027) and the U.S. Department of Energy, Office of Science, Office of Basic Energy Sciences, Division of Materials Science and Engineering (Grant No. DE-FG02-07ER46383 for T.-C.C.). The experiment was carried out as a joint research in the Synchrotron Radiation Research Organization and the Institute for Solid State Physics, the University of Tokyo (Proposal Nos. 2013B7454, 2014B7480, 2016A7503, and 2016B7523). T.-C.C. received a visiting professor appointment at the University of Tokyo during the experiment.

[1]A. K. Geim and I. V. Grigorieva, Nature **499**, 419 (2013).
[2]L. Y. Gan, Q. Zhang, Y. Cheng, and U. Schwingenschlögl, J. Phys. Chem. Lett. **5**, 1445 (2014).
[3]A. Jakubowicz, D. Mahalu, M. Wolf, A. Wold, and R. Tenne, Phys. Rev. B **40**, 2992 (1989).
[4]J. Buck, J. Iwicki, K. Rossnagel, and L. Kipp, Phys. Rev. B **83**, 75312 (2011).
[5]R. Schlaf, A. Klein, C. Pettenkofer, and W. Jaegermann, Phys. Rev. B **48**, 14242 (1993).
[6]M. Ogawa, S. Yamamoto, Y. Kousa, F. Nakamura, R. Yukawa, A. Fukushima, A. Harasawa, H. Kondoh, Y. Tanaka, A. Kakizaki, and I. Matsuda, Rev. Sci. Instrum. **83**, 23109 (2012).
[7]S. Yamamoto, Y. Senba, T. Tanaka, H. Ohashi, T. Hirono, H. Kimura, M. Fujisawa, J. Miyawaki, A. Harasawa, T. Seike, S. Takahashi, N. Nariyama, T. Matsushita, M. Takeuchi, T. Ohata, Y. Furukawa, K. Takeshita, S. Goto, Y. Harada, S. Shin, H. Kitamura, A. Kakizaki, M. Oshima, and I. Matsuda, J. Synchrotron Radiat. **21**, 352 (2014).
[8]J. M. Riley, W. Meevasana, L. Bawden, M. Asakawa, T. Takayama, T. Eknapakul, T. K. Kim, M. Hoesch, S.-K. Mo, H. Takagi, T. Sasagawa, M. S. Bahramy, and P. D. C. King, Nat. Nanotechnol. **10**, 1043 (2015).
[9]K. Osada, M. Tanaka, S. Ohno, and T. Suzuki, Jpn. J. Appl. Phys., Part 1 **55**, 65201 (2016).
[10]T. Finteis, M. Hengsberger, T. Straub, K. Fauth, R. Claessen, P. Auer, P. Steiner, S. Hüfner, P. Blaha, M. Vögt, M. Lux-Steiner, and E. Bucher, Phys. Rev. B **55**, 10400 (1997).

[11]W. Jaegermann, C. Pettenkofer, and B. A. Parkinson, Phys. Rev. B **42**, 7487 (1990).
[12]A. Klein, C. Pettenkofer, W. Jaegermann, M. Lux-Steiner, and E. Bucher, Surf. Sci. **321**, 19 (1994).
[13]N. Alidoust, G. Bian, S.-Y. Xu, R. Sankar, M. Neupane, C. Liu, I. Belopolski, D.-X. Qu, J. D. Denlinger, F.-C. Chou, and M. Z. Hasan, Nat. Commun. **5**, 4673 (2014).
[14]Y. Wang, J. M. Holden, A. M. Rao, P. C. Eklundt, U. D. Venkateswaran, D. Eastwood, R. L. Lidberg, G. Dresselhaus, and M. S. Dresselhaus, Phys. Rev. B **51**, 4547 (1995).
[15]R. F. Frindt, J. Phys. Chem. Solids **24**, 1107 (1963).
[16]S. M. Sze and K. K. Ng, *Physics of Semiconductor Devices*, 3rd ed. (John Wiley & Sons, Inc., Hoboken, New Jersey, 2007).
[17]L. Kronik and Y. Shapira, Surf. Sci. Rep. **37**, 1 (1999).
[18]D. Bröcker, T. Gießel, and W. Widdra, Chem. Phys. **299**, 247 (2004).
[19]A. B. Sproul, J. Appl. Phys. **76**, 2851 (1994).
[20]K. L. Luke and L. Cheng, J. Appl. Phys. **61**, 2282 (1987).
[21]K. Ozawa, S. Yamamoto, R. Yukawa, R. Liu, M. Emori, K. Inoue, T. Higuchi, H. Sakama, K. Mase, and I. Matsuda, J. Phys. Chem. C **120**, 29283 (2016).
[22]W. Shockley and W. T. Read, Jr., Phys. Rev. **87**, 835 (1952).